Liu, X., Zang, N., & Azarpeyvand, M. (2020). Control of Wake-Airfoil Interaction Noise Using Slotted-sawtooth Trailing-edge Serrations. In *AIAA Aviation 2020 Forum* https://doi.org/10.2514/6.2020-2517

Control of Wake-Airfoil Interaction Noise Using Slotted-sawtooth Trailing-edge Serrations

Xiao Liu*, B. Zang†, Mahdi Azarpeyvand‡
Faculty of Engineering, University of Bristol, BS8 1TR, United Kingdom.

This paper presents a study on the effectiveness of the application of a trailing-edge serration as a passive control method for reducing the wake-airfoil interaction noise from two airfoils in tandem. Two chambered airfoils, a NACA 65-(12)10 and a NACA 65-710 airfoil have been set up in tandem configuration in this study. To better understand the aerodynamic and aeroacoustic effects of wake interaction noise, an adjustment mechanism has been designed to allow free vertical movement of the rear airfoil. A slotted-sawtooth serration has been applied on the trailing-edge of the front airfoil as it has proven to be effective from our previous studies.[1] The rear airfoil was equipped with several pressure taps and surface pressure transducers. Far-field and near-field noise have been measured using the far-field microphone array and remote sensing probe technique. The results show that the use of slotted-sawtooth serration at the angle of incidence 10° can lead to a significant reduction of the far-field noise as the rear airfoil starts to interact with the wake of the front airfoil. The overall noise reduction level is up to 10dB, which is believed to be due to a faster turbulence kinetic energy decay of the wake from the serrated trailing-edge. Results have also shown that a significant reduction of surface pressure fluctuation and the near-field and far-field coherence can be achieved over the leading-edge area of the rear airfoil.

Nomenclature

c	chord length of the airfoil, mm
$2h$	amplitude of serration, mm
H	serration slot depth, mm
d	serration slot width, mm
λ	serration wavelength, mm
U_0	free-stream wind speed, m/s
Re_c	chord-based Reynolds number
x_g	gap distance between the front and rear airfoils in x direction, mm
y_g	gap distance between the front and rear airfoils in y direction, mm
α	angle of incidence of the airfoil, deg
kc	non-dimensionalized frequency, $2\pi fc/c_0$
c_0	speed of sound, m/s
f	frequency, Hz
SPL	Sound Pressure Level, dB
PSD	Power spectral density, dB/Hz

*Technical Specialist for Wind Tunnel Laboratory, Faculty of Engineering, University of Bristol. xiao.liu@bristol.ac.uk
†Research Associate, Faculty of Engineering, University of Bristol. nick.zang@bristol.ac.uk
‡Professor of Aerodynamics and Aeroacoustics, Faculty of Engineering, University of Bristol. m.azarpeyvand@bristol.ac.uk

I. Introduction

The noise produced by rotating blades is known to arise from the wake turbulent flow of the front-blade interacting with the rear-blade. Based on the findings of Boorks *et al.*,[2] this mechanism can be broadly categorized into trailing-edge, early separation and stall noise respectively. Over the past decades, the studies of the aerodynamic noise produced by the rotating blades have become a challenging task from both theoretical perspective and practical point of view. Many studies on the aerodynamic noise produced by the rotating blades has been carried out over the past decades. The mechanism of the noise generation by contra-rotating open rotor (CROR) propulsion systems were first investigated and analyzed in 1948 by Hubbard.[3] His study identified the dominant interference mechanisms and their associated noise production. Later, Hanson *et al.* reproduced and expanded Hubbard's findings by using turbofan theory.[4] For the contra-rotating open rotor (CROR) propulsion systems, the major source of noise is caused by the interaction of the tip and wake flow of the front propeller with the rear blades. Therefore, minimizing wake turbulence intensity of the front-blade should significantly affect the overall noise level of the CROR system. To reduce trailing-edge noise, several passive methods have been investigated extensively over the past decade, such as, trailing-edge serrations,[5–17] porous treatments,[18–22] surface treatments,[23,24] brushes[25,26] and morphing.[27,28] Serrated trailing-edges, in particular, have received significant interest due to its simple yet efficient noise reduction performance.

The efficiency of applying trailing-edge serrations for reducing noise have been investigated by Howe[29–31] extensively. Howe provided detailed analytical studies which showed that adding sawtooth and sinusoidal serrations on the trailing-edge of an airfoil will lead to the destructive sound interference which can significantly reduce the trailing-edge noise. However, Howe's mathematical model does not match the absolute noise reduction with the experimental data. More recently, Lyu *et al.*[32,33] improved Howe's existing analytical model by taking into account the existence of constructive sound interference in addition to the destructive sound interference predicted by Howe. A better agreement with the experimental data has then be observed from the results from the improved model. The implementation of trailing-edge serrations, such as sawtooth and slotted-sawtooth serrations, have studied by Gruber *et al.* and the results have shown that the use of sawtooth and slotted-sawtooth have superior noise reduction efficiency.[15] Later, The implementation of sawtooth and slotted-sawtooth serrated trailing-edge by Liu *et al.* have shown to be effective in reducing the wake turbulence intensity and the corresponding noise generation, especially at high angles of attack where maximum aerodynamic performance is obtained.[1,9–11] The ability of trailing-edge serration to reduce the turbulent energy content within the wake region can be associated with the highly three-dimensional flow originating from the tip- and root of the serration, making it an attractive solution to mitigate such wake-airfoil interaction noise for contra-rotating propellers and many other rotor-stator configurations.

Compared to the aeroacoustic studies of a single airfoil, fewer measurements have been reported on two airfoils aligned in tandem configurations. To expand the existing knowledge and better understand the effect of using trailing-edge serrations on the aerodynamic and aeroacoustic performance of wake-airfoil interaction, detailed of the near- and far-field noise measurements have been carried out and presented in this paper. By studying the dynamic pressure results on the rear airfoil from the remote sensing probe method, the effectiveness of a slotted-sawtooth trailing-edge serration on the wake-airfoil interaction noise has been investigated and compared with the straight (Baseline) trailing-edge airfoil. The experimental setup for the present study and the measurement techniques are discussed in section II. The results and discussions are provided in section III.

II. Experimental Setup

The present experiments were carried out using a cambered NACA 65(12)-10 airfoil and a NACA 65-710 airfoil in the aeroacoustic facility at the University of Bristol. The nozzle size of the tunnel is 0.775 m×0.5 m and capable of reaching reliable speeds of up to 40 m/s. The inflow velocity used for this study is $U_0 = 25$ m/s.

A. Airfoil and Serration Model Design Setup

The schematic of the tandem airfoils configuration set up with the trailing-edge serration is shown in Fig. 1(a). The front NACA 65-(12)10 airfoil were manufactured from aluminium-7075 and the rear NACA 65-710 airfoil is made by RAKU-TOOL WB-1222 polyurethane board. Both of the airfoils are machined using a computer numerical control (CNC) machine. At the trailing-edge of the front airfoil, a 2.3 mm blunt with a 15 mm

(h_b) depth and 0.8 mm thick slot along the span of the airfoil has been cut in order to install the flat plate (baseline case) and the slotted-sawtooth serration. In the previous experimental studies, the use of slotted-sawtooth serrations show clear noise and turbulent kinetic energy reduction.[9–11,15] The slotted-sawtooth serration used in this study with geometrical parameters of the amplitude $2h = 30$ mm, periodicity wavelength $\lambda = 9$ mm, the slot width $d = 0.5$ mm and slot depth $H = 15$ mm (Fig. 1(b)). The rear airfoil, was equipped with a total number of 34 ports on both the pressure and suction sides of the airfoil for the static and dynamic pressure measurement, see Fig. 1(a).

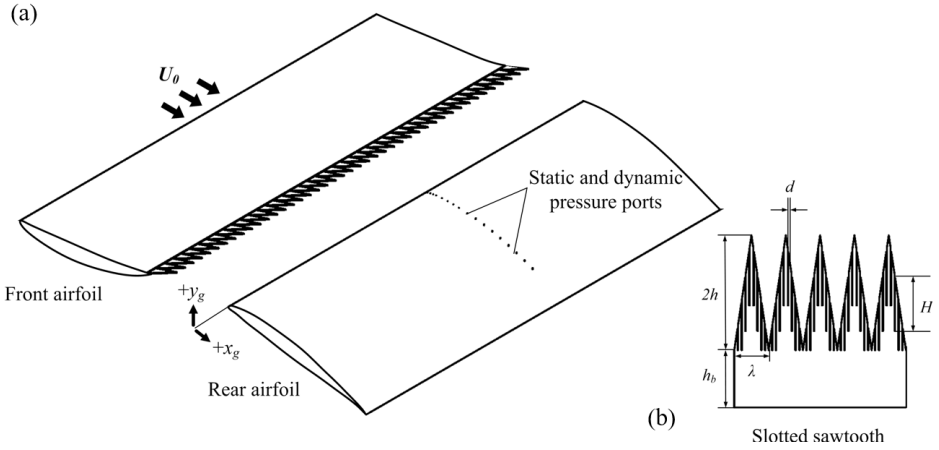

Figure 1: Tandem airfoil set up, (a) Tandem airfoil configuration (b) geometrical parameters of the slotted sawtooth serration.

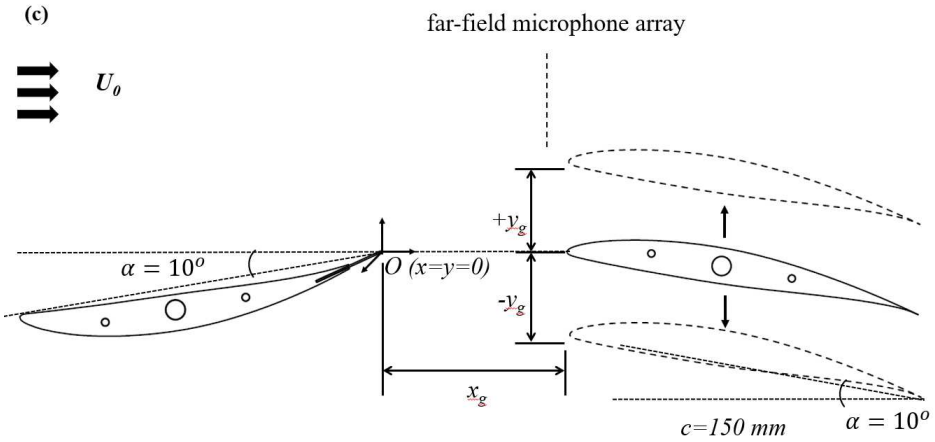

Figure 2: Side view of the tandem airfoil configuration.

A total number of 20 remote sensors, 15 on the suction side and 5 on the pressure side were populated on the rear airofoil. These remote sensors were use to capture the unsteady surface pressure fluctuation with a frequency range from 50Hz to 15kHz. All the remote sensing microphones were calibrated by a G.R.A.S. 40PL microphone according to the procedures described by Mish *et al.* and Elsahhar *et al.*[34,35] This remote sensing technique and the calibration procedures have also been used by Mayer *et al.*[36,37] to study the airfoil trailing-edge noise in static and dynamic conditions. A far-field microphone array with a total number of 23 G.R.A.S. microphone has been set up around 1.75 m above the leading-edge of the rear airfoil. The synchronous remote sensor and far filed measurements were acquired with National Instruments PXIe-4499 data acquisition modules at a sampling rate of 2^{16} Hz for 16 seconds. The power spectral density (PSD) and sound pressure level (SPL) of the near-field pressure fluctuations and farfield noise were later post-processed

by applying Welch function with a window size of 2^{13} and 50% overlap. The frequency resolution, i.e. bin size, was kept constant at 8Hz.

Both airfoils have been set to angles of insicidence of 10° (Fig. 2) which the serration produces better TKE decay in the airfoil wake.[1,10,11,38] The two airfoils are placed parallel to each other, in a uniform flow, and rectangular end-plates are fixed on the side of the nozzle to maintain a nearly two-dimensional flow over the two airfoils. Adjustment mechanism has been designed to allow placement of the rear airfoil in two horizontal locations ($x_g = 0.3c$ and $0.5c$) and free vertical movement ($y_g = \pm 0.4c$). Note that, x_g and y_g were defined based on the trailing-edge of the front airfoil with $h = 15$ mm flat plate(Baseline case).

III. Results and Discussion

A. Far-field acoustic Measurements

As presented in the previous study by Liu *et. al*, placing a rear airfoil in tandem will lead to significant changes to the wake of the front airfoil.[38] In order to further investigate the effectiveness of trailing-edge serration treatments for reducing the wake-airfoil interaction noise, detailed far-field measurement has been carried out using far-field microphone array. The rear airfoil while fixed at either $x_g = 0.3c$ or $0.5c$ in horizontal distance, is traversed in the vertical direction with a step size of $\delta y_g = 2$ mm to cover the entire front airfoil wake (from $y_g = -0.1c$ to $0.4c$).

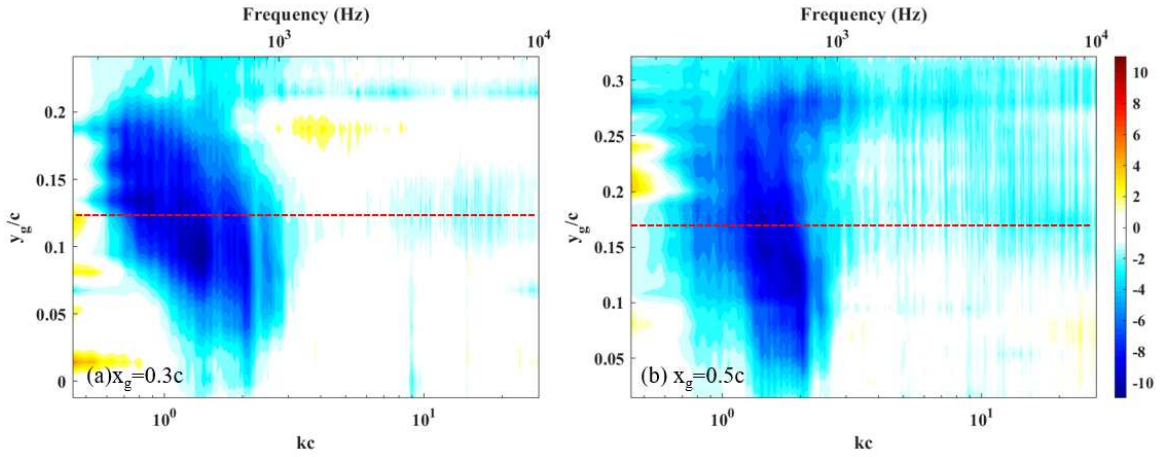

Figure 3: Contour maps of the PSD difference between serrated and unserrated case ($\triangle PSD$) for tandem airfoil with horizontal gap distance (a)$x_g = 0.3c$ and (b)$x_g = 0.5c$ and wide range of vertical gap distance y_g. Notes that the red line allocate the vertical gap location where maximum noise reduction observed.

Far-field noise difference between the serrated case and the Baseline case(ΔPSD) have been calculated ($\Delta PSD = PSD_{serrated} - PSD_{baseline}$) and plotted in the contour maps in Fig. 3, while the y_g/c represents the vertical locations of the rear airfoil. Noted that a negative difference (in blue) represents noise reduction and vice versa. In Figs. 3(a) and (b), for two horizontal locations, $x_g = 0.3c$ and $0.5c$, noise reduction can be observed from frequencies of approximately $f = 200$Hz to 1000Hz as the rear airfoil moves through the wake. This corresponds to the non-dimensional frequency number range of $0.5 > kc > 3$, where $kc = 2\pi fc/c_0$ with c_0 refers to the speed of sound. As the rear airfoil gradually moved into the wake region of the front airfoil from around $y_g = 0.02c$ and $y_g = 0.03c$ for $x_g = 0.3c$ and $0.5c$, the noise reduction becomes more significant in both the magnitude and the frequencies range. As shown in Figs. 3(a), a maximum noise reduction of above 10dB can be observed over $0.5 \leq kc \leq 3$ (200Hz $< f <$ 1000Hz) at $x_g/c = 0.3$ and $y_g/c = 0.13$. For $x_g/c = 0.5$ in Fig. 3(b), a even greater noise reduction (above 12dB) can be observed over $0.5 \leq kc \leq 4$ (200Hz $< f <$ 1000Hz) at $y_g/c = 0.17$. From ealier study by Gruber *et al.*,[15] kc range ($0.5 > kc > 5$), has been identified as the region dominated by turbulence interaction noise and $kc > 5.5$ has been identified as trailing-edge self-noise for tandem airfoil configurations, at similar Reynolds number.

The far-field noise results at vertical gap location where maximum noise reduction observed (in red line in Fig. 3) have then been presented in Fig. 4. For reference, the background noise is shown in grey in the

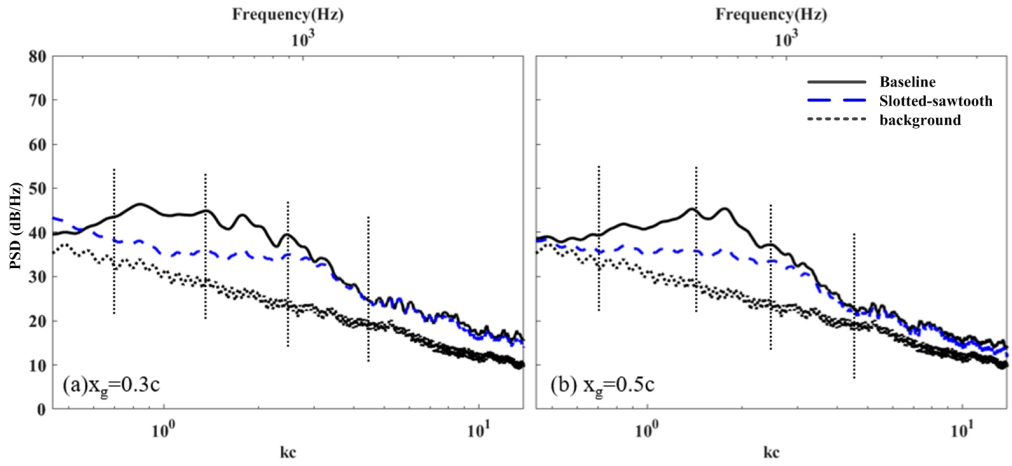

Figure 4: Fairfield power spectral density of the interrelation noise with airfoil gap distance of (a) $x_g = 0.3c$, $y_g = 0.26c$ and (b) $x_g = 0.5c$, $y_g = 0.67c$, black solid line: Baseline, blue dash line: Slotted-sawtooth serrated, black dot line: background.

figures. In Fig. 4(a), when compared with the Baseline case, the far-field PSD demonstrates that the use of trailing-edge serration on front airfoil can lead to a clear decrease (up to 11 dB/Hz) in the far-field noise within the frequency range of $0.5 < kc < 3$. At a higher frequency range ($kc > 3$) the far-field PSD for the serrated case resulted in a similar magnitude and trend, as the Baseline case. When increasing the horizontal distance between two airfoils x_g to $0.5c$ (see Fig. 4(b)), the result show similar behaviour as the case for $x_g = 0.3c$ with the maximum noise reduction up to around 12 dB/Hz.

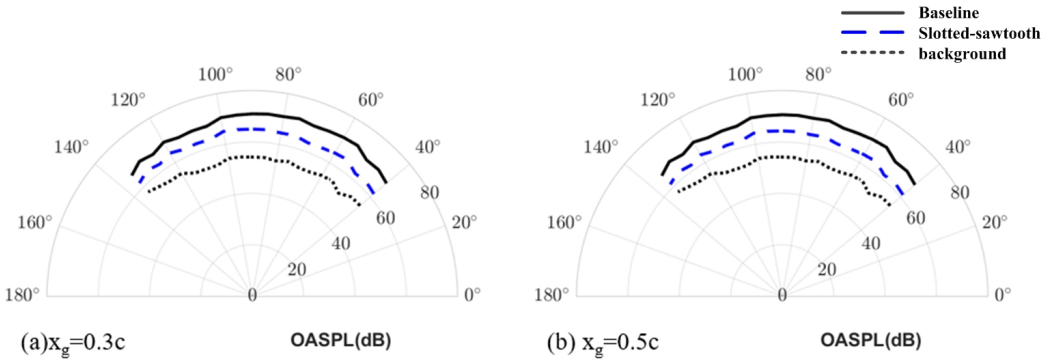

Figure 5: Overall sound pressure levels and directivity of the interaction noise with airfoil gap distance of (a)$x_g = 0.3c$ and (b)$x_g = 0.5c$, black solid line: Baseline, blue dash line: Slotted-sawtooth serrated, black dot line: background.

Figure 5 presents the overall sound-pressure-level (OASPL) and its directivity pattern for the Baseline and slotted-sawtooth serrated cases for two different horizontal gap distances ($x_g = 0.3c$ in Fig. 5(a) and $0.5c$ in Fig. 5(b)) at the vertical gap distances, y_g, where the maximum far-field noise reduction is attained. As shown in the figures, substantial overall noise reduction can be obtained with the use of slotted-sawtooth case with approximately 7dB at all polar angles for $x_g = 0.3c$, and the reduction improves further to 10dB for the larger x_g.

Based on the result in Fig. 4, four different kc values, at the low frequency (beginning of the reduction region $kc = 0.7$), the mid-frequencies (the frequency within the reduction region $kc = 1.4$ and 2.5) and the high frequency (higher than the reduction region $kc = 4.4$) have been chosen to examine the frequency-

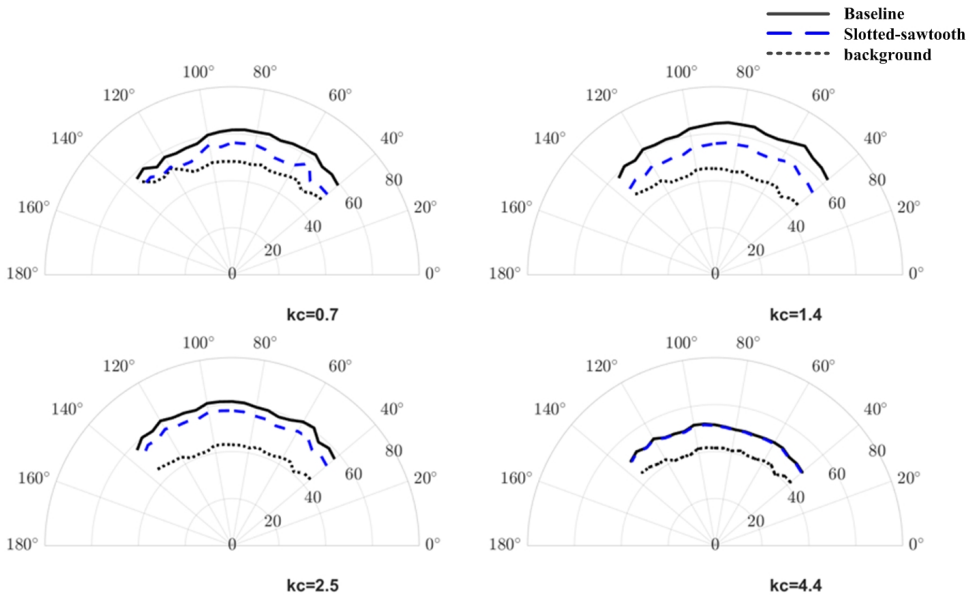

Figure 6: One-third octave band sound pressure levels and directivity of the interactions with airfoil gap distance of $x_g = 0.3c$ and $y_g = 0.26c$, black solid line: Baseline, blue dash line: Slotted-sawtooth serrated, black dot line: background.

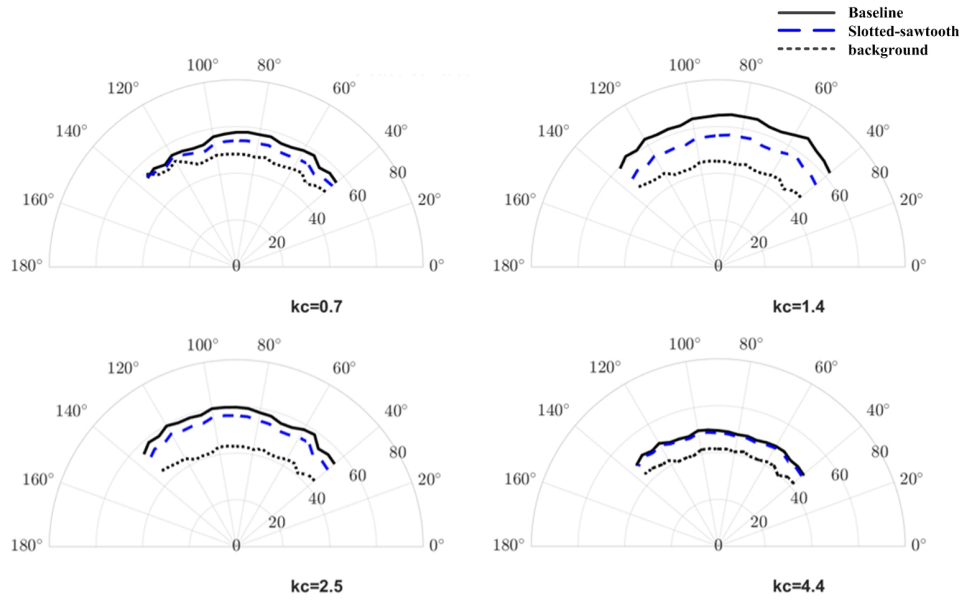

Figure 7: One-third octave band sound pressure levels and directivity of the interactions with airfoil gap distance of $x_g = 0.5c$ and $y_g = 0.67c$, black solid line: Baseline, blue dash line: Slotted-sawtooth serrated, black dot line: background.

dependent changes in both far-field noise level and directivity. As shown in Figs. 6 and 7, for both $x_g/c = 0.3$ and 0.5 cases, it is clear that the directivity of the radiated far-field noise for the serrated cases shows similar pattern to that of the Baseline cases for all selected kc values. In the result of low to middle kc values, $kc = 0.7$, 1.4 and 2.5 in Figs. 6(a) to (c) and Figs. 7(a) to (c), for both two horizontal gap distances, clear

reduction of the sound pressure level in all directions can be observed when the slotted-sawtooth serration is applied to the front airfoil trailing-edge in the results of the serrated cases. Moreover, the difference between the Baseline and the serrated airfoils gradually increases while the polar angle increases, i.e. moving from upstream to downstream.

B. Nearfield Measurements

Knowing that the use of slotted-sawtooth can resulting substantial reduction of the far-field noise, it is now useful to examine the near-field unsteady loading on the rear airfoil since it provides a measurement of the turbulent flow impinging directly upon the rear airfoil. The surface pressure fluctuation measurements have been performed on the rear airfoil and correlate it with the far-field noise results. A flat plate (Baseline) and a slotted-sawtooth serration was applied on the trailing-edge of the front airfoil and the surface pressure fluctuation on the rear airfoil have been acquired using remote sensor microphones. The rear airfoils were placed at the vertical locations where the rear airfoil interact most notably with the wake of the front airfoil, which is $y_g = 0.13c$ and $0.17c$ for gap distance between two airfoil $x_g = 0.3c$ and $0.5c$, respectively. Figures 8 and 9 depict the surface pressure fluctuation PSD along both the suction sides of the rear airfoil at $x_g = 0.3c$ and $0.5c$. Note that figures are arranged in a way that it starts from the pressure measurement locations at the pressure side and follow a clockwise sense of rotation with reference to the quarter chord of the rear airfoil, all the way to the last measurement point on the suction side.

As shown in Fig. 8, a broadband hump in the non-dimensional frequency range of around $0.55 < kc < 2.75$ can be observed in the result for the Baseline case (in black solid line), especially close to the leading-edge on both the pressures side (Fig. 8(a) to (d)) and suction side (Fig. 8(e) to (k)). However, when the slotted-sawtooth serration is applied on the trailing-edge of the front airfoil (in blue dash line), a significant surface pressure fluctuation PSD reduction can be found in the hump region. The maximum PSD reduction magnitude is about 9 dB/Hz. For higher frequency range, $kc > 2.75$, the result for serrated case on the pressure side show a slight increase in the PSD level in the Fig. 8(a), while close to the leading-edge of the airfoil 8(b) to (d), surface pressure fluctuation PSD of the serrated case resulted in a small reduction. On the suction side of the airfoil, it is almost negligible and minor decrease in the higher frequency range, especially close to the leading-edge of the airfoil can be observed. For the result at larger x_g in Fig 9, it is shown that the use of the trailing-edge serration can lead to a clear reduction of the surface pressure fluctuation PSD, especially around the leading-edge of the rear airfoil with the kc range between 0.55 to 2.75, similar the that of smaller x_g. The result for serrated case for higher frequency also show an approximate of 2 dB/Hz lower than that of the Baseline case at most of the locations around the leading-edge of the rear airfoil.

It is interesting that the frequency range observed with most significant reduction in the surface pressure PSD, $0.55 < kc < 2.75$, agrees very well with the frequency range of far-field noise reduction. In the previous study, applying a slotted-sawtooth serration on the trailing-edge of an airfoil has proven to be able to lead to a wake velocity deficit as well as a great reduction of the turbulent kinetic energy level in the downstream wake region as compared to the Baseline case.[1,11] Since the wake-airfoil intereaction noise is directly related to the surface pressure fluctuations due to the wake turbulence of the front airofil hitting on the leading-edge of the rear airfoil, therefore, a lower wake turbulence can possibly lead to a smaller unsteady aerodynamic loading on the leading-edge area of the rear airfoil, and hence the overall noise reduction across the range of frequencies.[39]

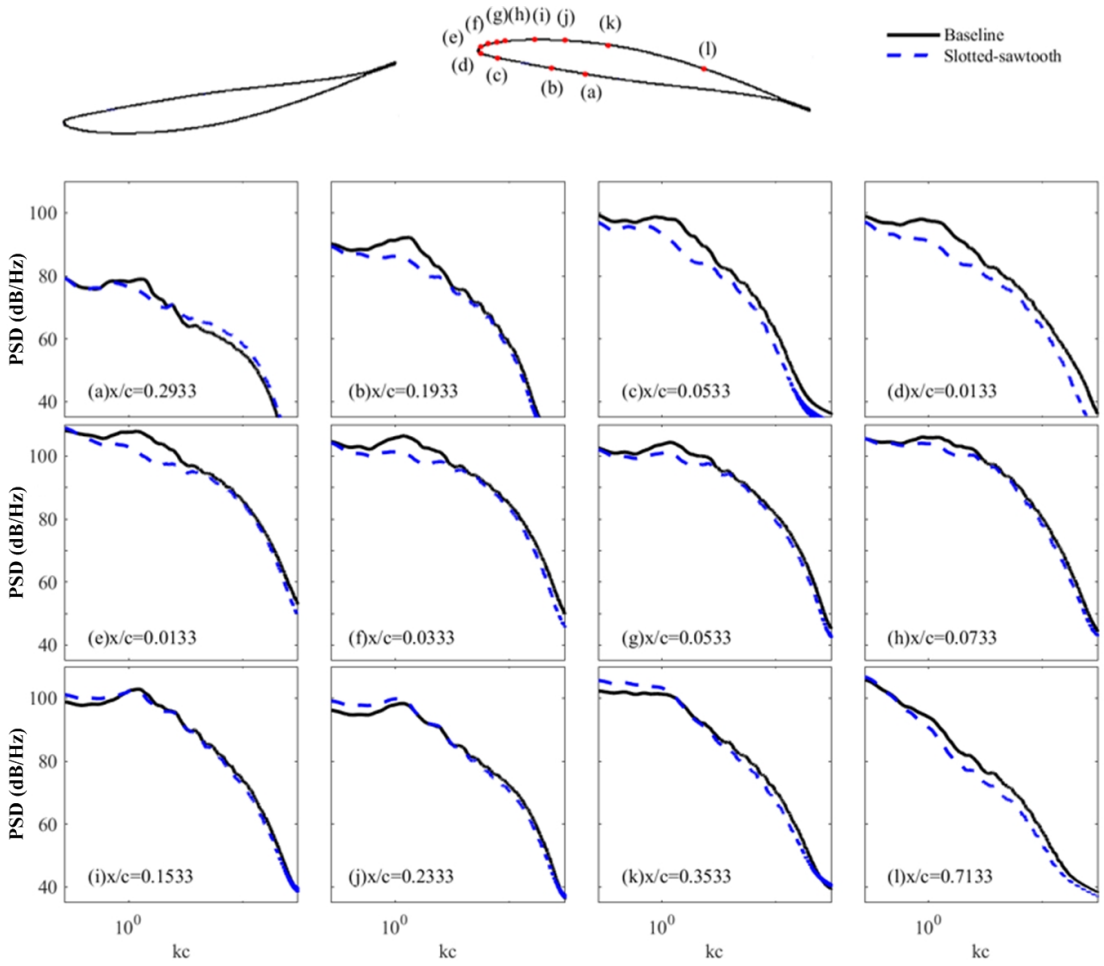

Figure 8: Power spectral density of surface pressure fluctuation on the rear airfoil at $\alpha = 10^\circ$ and location $x_g = 0.3c$ and $y_g = 0.26c$, black solid line: Baseline, blue dash line: Slotted-sawtooth serrated

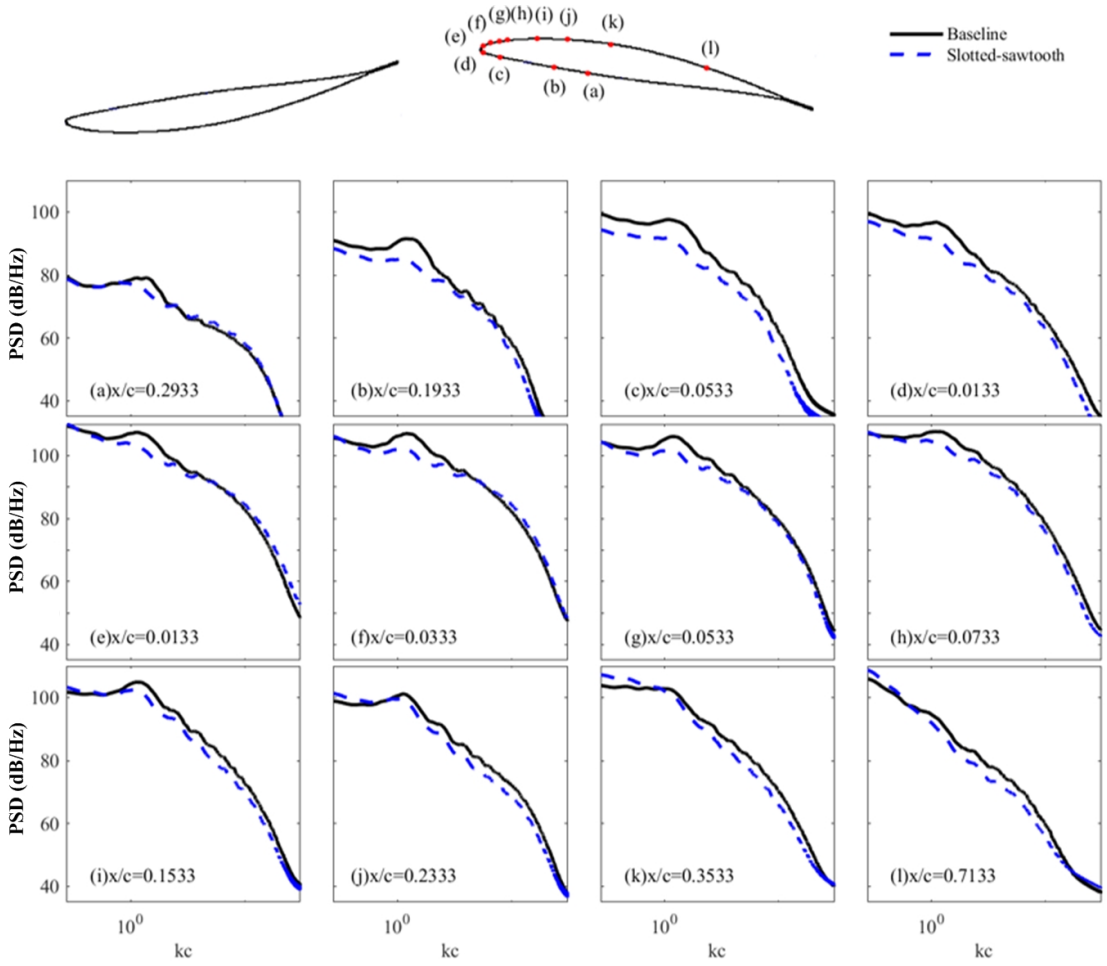

Figure 9: Power spectral density of surface pressure fluctuation on the rear airfoil at $\alpha = 10°$ and location $x_g = 0.5c$ and $y_g = 0.67c$, black solid line: Baseline, blue dash line: Slotted-sawtooth serrated

C. Near-field and Far-field Coherence

Based on the study by Lacagnina *et al.*,[40] simultaneous measurement of unsteady pressure fluctuation for near- and far-field proves to be effective and useful to directly relate the near-field surface pressure fluctuation and far-field radiated noise. In order to better illustrate the effect of trailing-edge serration on the wake turbulence interaction with the leading-edge of the rear airfoil, the coherence between the unsteady pressure from all surface pressure measurement points on the suction side of the rear airfoil and the 90° far-field microphone has been determined as:

$$\gamma^2(f) = \frac{|\phi_{pi,pj}(f)|^2}{\phi_{pi,pi}(f)\phi_{pj,pj}(f)}, \tag{1}$$

where ϕ_{pp} is the Fourier-transformed pressure fluctuation spectra. The coherence contour maps are presented in Figs. 10 and 11 for $x_g = 0.3c$ and $0.5c$. The positive x/c represents the coherence results along the suction side of the rear airfoil ($x/c = 0$ is leading-edge of the airfoil).

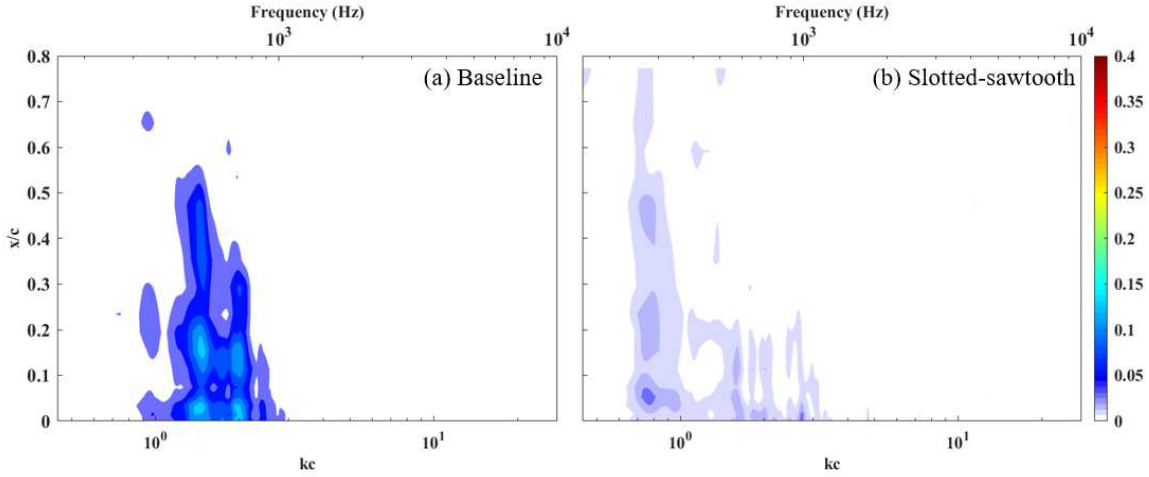

Figure 10: Contour map of coherence (γ^2) between the near-field microphones on suction side of the rear airfoil with the 90^o far-field microphone at horizontal gap distance $x_g = 0.3c$.

The coherence map for the Baseline case for both two x_g locations (Fig.10(a) and 11(a))show a high coherence region in the frequency range ($0.9 < kc < 2$) and this high coherence region occurs from leading-edge to till $0.7c$ of the suction side of the rear airfoil. This region also agree approximately with the broadband hump which is believed due to the wake-airfoil interaction in both the near-field surface pressure fluctuation (see Figs. 8 and 9) and far-field noise spectra (see Fig. 4) in previous sections. In Figs.10(b) and 11(b), when applying slotted-sawtooth serration on the trailing-edge of the front airfoil, a clear loss of coherence can be observed between the near- and far-field pressure fluctuations compared with the baseline case. Also the frequency range of the near- and far-field coherence expend to a wider frequency range, $0.7 < kc < 4$ for the case with smaller gap distance $x_g = 0.3c$ and $0.7 < kc < 2.5$ for the case of $x_g = 0.5c$. This possible suggests that a wider range of turbulent structure correlated with the far-field noise with the use of slotted-sawtooth serration. Similar reduction trend again can be found in the near-field surface pressure fluctuation and far-field noise spectra. More importantly, this agreement again show a hint that the interaction noise between the wake turbulence and leading-edge of the rear airfoil is indeed can be seen as a primary source of the far-field radiated noise, furthermore, the near-field surface pressure fluctuation at the leading-edge locations is directly related to the generation of wake- airfoil interaction noise.

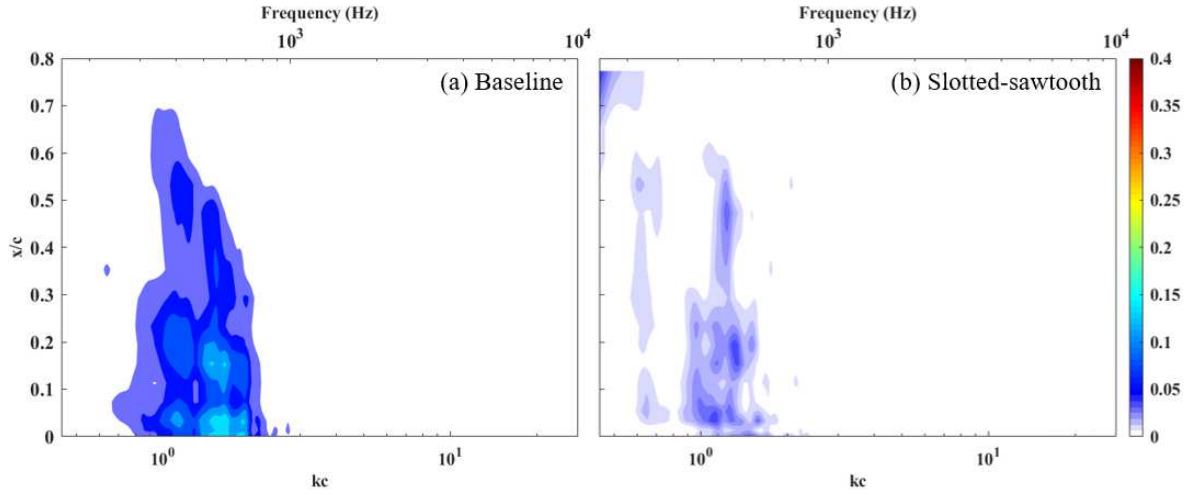

Figure 11: Contour map of coherence (γ^2) between the near-field microphones on suction side of the rear airfoil with the 90^o far-field microphone at horizontal gap distance $x_g = 0.5c$.

IV. Conclusion

Effects on the passive control of wake-airfoil interaction noise with the application of a slotted-sawtooth serration on the trailing-edge of a NACA 65-(12)10 airfoil which has been set up in tandem configurations with another NACA 65-710 has been examined in this study. Adjustment mechanism on the rear airfoil for a free vertical movement was used to facilitate the detailed aerodynamic and aeroacoustic measurement of the rear airfoil moving from outside of the front arifoil wake to inside of the front airfoil wake position. The results show that, at the angle of incidence 10°, a significant reduction of the far-field noise can be observed for the slotted-sawtooth serration case when the rear airfoil starts to interact with the wake of the front airfoil. The overall noise reduction level is up to more than 10 dB for both horizontal distances tested, over the frequency range of $0.5 < kc < 2.74$. The near-field measurements also demonstrate a clear reduction of surface pressure fluctuation PSD over a comparable frequency range. The near-field to far-field coherence show that comparing to the Baseline case, the slotted-sawtooth serration both reduces the extent of coherence between the near-field and far-field pressure fluctuations and expends the frequency range of the coherence. This present results show that the wake-airfoil interaction noise can be seen as a primary source of the far-field radiated noise for tandem airfoils configuration and give a hint that the reduction in near-field unsteady loading of the rear airfoil can lead to reduction of the radiated noise.

References

[1]Liu, X., Kamliya Jawahar, H., Azarpeyvand, M., and Theunissen, R., "Aerodynamic performance and wake development of airfoils with serrated trailing-edges," *AIAA Journal*, Vol. 55, No. 11, 2017, pp. 3669–3680.

[2]Brooks, T., Pope, D., and Marcolini, M., "Airfoil Self-Noise and Prediction," *NASA-RP-1218*, 1989.

[3]Hubbard, H. H., "Sound from dual-rotating and multiple single-rotating propellers," Naca technical note 1654, Langley Aeronautical Laboratory, Langley Field, Va., United States, 1948.

[4]Hanson D. B., "Noise of Counter-Rotation Propellers," *Journal of Aircraft*, Vol. 22, No. 7, 1985, pp. 609–617.

[5]Sandberg, R. and Jones, L., "Direct numerical simulations of low Reynolds number flow over airfoils with trailing-edge serrations," *Journal of Sound and Vibration*, Vol. 330, No. 16, 2011, pp. 3818–3831.

[6]Moreau, D., Brooks, L., and Doolan, C., "On the noise reduction mechanism of a flat plate serrated trailing edge at low-to-moderate Reynolds number," *18th AIAA/CEAS aeroacoustics conference (33rd AIAA aeroacoustics conference)*, AIAA 2012-2186.

[7]Chong, T., Joseph, P., and Gruber, M., "Airfoil self noise reduction by non-flat plate type trailing edge serrations," *Applied Acoustics*, Vol. 74, No. 4, 2013, pp. 607–613.

[8]Ji, L., Qiao, W., Tong, F., Xu, K., and Chen, W., "Experimental and numerical study on noise reduction mechanisms of the airfoil with serrated trailing edge," *20th AIAA/CEAS Aeroacoustics Conference*, AIAA 2014-3297.

[9]Liu, X., Azarpeyvand, M., and Theunissen, R., "Aerodynamic and aeroacoustic performance of serrated airfoils," *21st AIAA/CEAS Aeroacoustics Conference*, AIAA 2015-2201.

[10]Liu, X., Azarpeyvand, M., and Theunissen, R., "On the Aerodynamic Performance of Serrated Airfoils," *22nd International Congress on Sound and Vibration*, 2015, pp. 12–16.

[11]Liu, X., Kamliya Jawahar, H., Azarpeyvand, M., and Theunissen, R., "Wake development of airfoils with serrated trailing edges," *22nd AIAA/CEAS Aeroacoustics Conference*, AIAA 2016-2817.

[12]Avallone, F., Arce Leon, C., Pröbsting, S., Lynch, K. P., and Ragni, D., "Tomographic-PIV investigation of the flow over serrated trailing-edges," *54th AIAA Aerospace Sciences Meeting*, AIAA 2016-1012.

[13]Chong, T. P. and Joseph, P. F., "An experimental study of airfoil instability tonal noise with trailing edge serrations," *Journal of Sound and Vibration*, Vol. 332, No. 24, 2013, pp. 6335–6358.

[14]Azarpeyvand, M., Gruber, M., and Joseph, P., "An analytical investigation of trailing edge noise reduction using novel serrations," *19th AIAA/CEAS aeroacoustics conference*, AIAA 2013-2009.

[15]Gruber, M., "Airfoil noise reduction by edge treatments," *Thesis, University of Southampton*, 2012.

[16]Gruber, M., Azarpeyvand, M., and Joseph, P. F., "Airfoil trailing edge noise reduction by the introduction of sawtooth and slitted trailing edge geometries," *integration*, Vol. 10, 2010, pp. 6.

[17]Gruber, M., Joseph, P., and Azarpeyvand, M., "An experimental investigation of novel trailing edge geometries on airfoil trailing edge noise reduction," *19th AIAA/CEAS Aeroacoustics Conference*, A1AA 2013-2011.

[18]Vathylakis, A., Chong, T. P., and Joseph, P. F., "Poro-serrated trailing-edge devices for airfoil self-noise reduction," *AIAA Journal*, Vol. 53, No. 11, 2015, pp. 3379–3394.

[19]Showkat Ali, S. A., Szoke, M., Azarpeyvand, M., and Ilário, C., "Trailing Edge Bluntness Flow and Noise Control Using Porous Treatments," *22nd AIAA/CEAS Aeroacoustics Conference*, AIAA 2016-2832.

[20]Showkat Ali, S. A., Azarpeyvand, M., Szőke, M., and da Silva, C. R., "Boundary layer flow interaction with a permeable wall," *Physics of Fluids*, Vol. 30, No. 8, 2018, pp. 085111.

[21]Showkat Ali, S. A., Szőke, M., Azarpeyvand, M., and Ilario da Silva, C. R., "Turbulent Flow Interaction with Porous Surfaces," *24th AIAA/CEAS Aeroacoustics Conference*, 2018-2801.

[22]Showkat Ali, S. A., Azarpeyvand, M., and da Silva, C. R., "Trailing-edge flow and noise control using porous treatments," *Journal of Fluid Mechanics*, Vol. 850, 2018, pp. 83–119.

[23]Afshari, A., Azarpeyvand, M., Dehghan, A. A., and Szőke, M., "Trailing Edge Noise Reduction Using Novel Surface Treatments," *22nd AIAA/CEAS Aeroacoustics Conference*, AIAA 2016-2384.

[24]Afshari, A., Azarpeyvand, M., Dehghan, A. A., Szőke, M., and Maryami, R., "Trailing-edge flow manipulation using streamwise finlets," *Journal of Fluid Mechanics*, Vol. 870, 2019, pp. 617–650.

[25]Herr, M. and Dobrzynski, W., "Experimental Investigations in Low-Noise Trailing Edge Design." *AIAA journal*, Vol. 43, No. 6, 2005, pp. 1167–1175.

[26]Finez, A., Jacob, M., Jondeau, E., and Roger, M., "Broadband noise reduction with trailing edge brushes," *16th AIAA/CEAS Aeroacoustics Conference*, AIAA 2010-3980.

[27]Ai, Q., Azarpeyvand, M., Lachenal, X., and Weaver, P. M., "Aerodynamic and aeroacoustic performance of airfoils with morphing structures," *Wind Energy*, Vol. 19, No. 7, 2016, pp. 1325-1339.

[28]Ai, Q., Azarpeyvand, M., Lachenal, X., and Weaver, P. M., "Airfoil noise reduction using morphing trailing edge," *21st International Congress on Sound and Vibration*, 2014.

[29]Howe, M. S., "A Review of the Theory of Trailing Edge Noise," *Journal of Sound and Vibration*, Vol. 61, No. 3, 1978, pp. 437–465.

[30]Howe, M. S., "Noise Produced by a Sawtooth Trailing Edge," *Journal of the Acoustical Society of America*, Vol. 90, No. 1, 1991, pp. 482–487.

[31]Howe, M. S., "Aerodynamic Noise of a Serrated Trailing Edge," *Journal of Fluids and Structures*, Vol. 5, No. 1, 1991, pp. 33–45.

[32]Lyu, B., Azarpeyvand, M., and Sinayoko, S., "A trailing-edge noise model for serrated edges," *21st AIAA/CEAS Aeroacoustics Conference*, 2015-2362.

[33]Lyu, B., Azarpeyvand, M., and Sinayoko, S., "Prediction of Noise from Serrated Trailing-Edges," *Journal of Fluid Mechanics*, Vol. 793, 2016, pp. 556–588.

[34]Mish, P. F., *An experimental investigation of unsready surface pressure on single and multiple airfoils*, Ph.D. thesis, Virginia Polytechnic Institute and State University, 2013.

[35]Elsahhar, E., Showkat Ali, S. A., Raf, T., and Azarpeyvand, M., "An experimntal investigation of the effect of bluff body bluntness factor on wake-vortex noise generation," *24th AIAA/CEAS Aeroacoustics Conference*, 2018, 2018-3288.

[36]Mayer, Y. D., Zang, B., and Azarpeyvand, M., "Aeroacoustic characteristics of a NACA 0012 airfoil for attached and stalled flow conditions," *25th AIAA/CEAS Aeroacoustics Conference*, 2019, 2019-2530.

[37]Mayer, Y. D., Zang, B., and Azarpeyvand, M., "Design of a Kevlar-walled test section with dynamic turntable and aeroacoustic investigation of an oscillating airfoil," *25th AIAA/CEAS Aeroacoustics Conference*, 2019, 2019-2464.

[38]Liu, X., Showkat Ali, S. A., Azarpeyvand, M., and Mayer, Y., "Aeroacoustic and aerodynamic study of trailing-edge serrated airfoils in tandem configuration," *23rd International Congress on Acoustics*, 2019.

[39]Amiet, R. K., "Acoustic radiation from an airfoil in a turbulent stream," *Journal of Sound and Vibration*, Vol. 41, No. 4, 1975, pp. 407 – 420.

[40]Lacagnina, G., Chaitanya, P., Berk, T., Kim, J.-H., Joseph, P., Ganapathisubramani, B., Hasheminejad, S. M., Chong, T. P., Stalnov, O., Choi, K.-S., Shahab, M. F., Omidyeganeh, M., and Pinelli, A., "Mechanisms of airfoil noise near stall conditions," *Physical Review Fluids*, Vol. 4, No. 12, 2019, pp. 123902.